

## Experimental and theoretical studies on new 7-(3,6-di-*tert*-butyl-9*H*-carbazol-9-yl)-10-alkyl-10*H*-phenothiazine-3-carbaldehydes

Kesavan Stalindurai, Kannan Gokula Krishnan, Erumaipatty Rajagounder Nagarajan,  
Chennan Ramalingan\*

*Department of Chemistry, Kalasalingam University, Krishnankoil, 626 126, Tamilnadu, India*

### ARTICLE INFO

#### Article history:

Received 28 June 2016

Received in revised form

19 October 2016

Accepted 6 November 2016

Available online xxx

#### Keywords:

Carbazole

Phenothiazine

GIAO

Polarizabilities

Hyperpolarizabilities

### ABSTRACT

Synthesis of fused heterocyclic aldehydes with carbazole (CZ) structural motif linked at C-7 position on phenothiazines (PTZ), 7-(3,6-di-*tert*-butyl-9*H*-carbazol-9-yl)-10-butyl-10*H*-phenothiazine-3-carbaldehyde (**1**) and 7-(3,6-di-*tert*-butyl-9*H*-carbazol-9-yl)-10-hexyl-10*H*-phenothiazine-3-carbaldehyde (**2**) has been accomplished and are characterized through experimental and computational techniques. The optimized structure with their bonding aspects and vibrational frequencies of the same have been examined utilizing DFT-B3LYP technique with a basis set 6-311++G(d,p). In the optimized structures of **1** and **2**, the bond lengths and bond angles are in accord with their corresponding reported analogous. The vibrational frequencies resulted from experimental as well as theoretical are in well accord with each other. Further, the results of polarizabilities, first order hyperpolarizabilities and dipole moment of **1** and **2** imply that these could be utilized for the preparation of NLO crystals which might generate second order harmonic waves.

© 2016 Elsevier B.V. All rights reserved.

### 1. Introduction

Carbazole (CZ), also branded as 9-azafluorene, and its derivatives are incredibly significant nitrogen possessing heteroaromatic compounds, which have been used as potential building blocks in the construction of a wide range of functional materials [1]. Besides, the CZ structural scaffold has been found in several bio-important chemical entities and exhibit antifungal [2], antibacterial [3], anti-inflammatory [4], antiviral [5], and antitumor properties [6]. Alkyl functionalized carbazoles play noteworthy roles in electron transport materials/dye-sensitized solar cells. For instance, it is known that CZ is an electron donor because of the existence of lone pair of electrons on the nitrogen. Since alkyl groups are electron donors in nature through inductive effect, incorporation of such groups on the CZ structural motif enhances the electron donating ability of the CZ unit. Further, introduction of alkyl groups helps in enhancing the materials solubility as well.

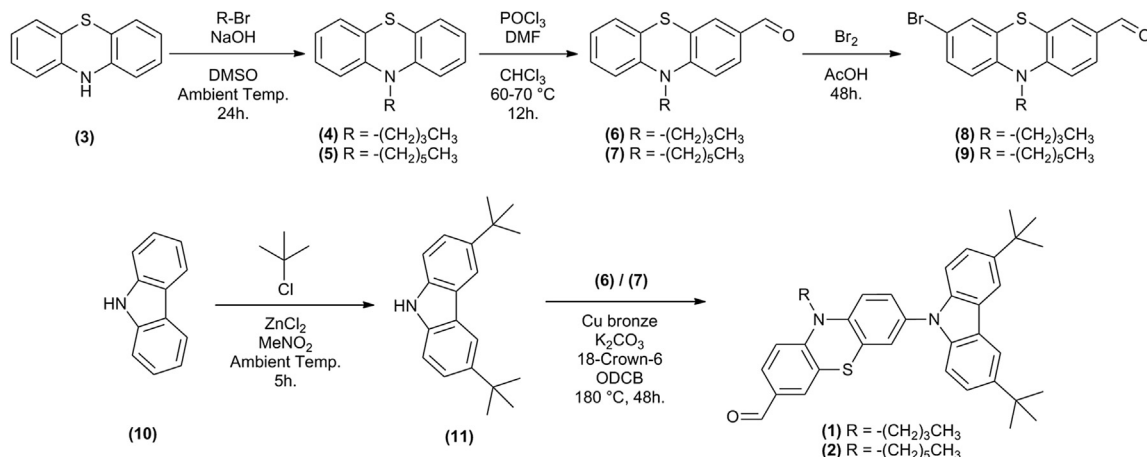
Phenothiazine (PTZ) and its derivatives are one of the classes of outstanding heterocyclic compounds with excellent electron donating nature and hence these trigger researchers to focus their

attention towards electro-chemical [7] and electro-optical properties [8]. They are widely used as potential intermediates in chemical manufacturing and active components of organic light emitting diodes (OLEDs) [9], semiconductors [10] and solar cells [11]. Besides their potential applications in materials science, PTZ has been utilized to construct chemical entities of biological significance which display various activities including anti-malarial [12], anti-cancer [13], anti-helminthic [14], anti-histamine [15] and anti-psychotic activity [16].

The wide variety of applications of organic molecules possessing CZ and PTZ structural motifs reported in the literature inspired us to focus our attention towards new systems carrying these two carbazole-phenothiazine moieties. We herein report synthesis as well as experimental and computational studies on compounds **1** and **2**. Structural parameters (optimized) were obtained by the calculations of density functional theory (DFT) with a basis set B3LYP/6-311++G(d,p). From the theoretical results, vibrational assignments and optimized structural parameters are deduced and these outcomes are correlated with the experimental results. The theoretical outcomes are found to be appreciably comparable with the experimental results.

\* Corresponding author.

E-mail address: [ramalinganc@gmail.com](mailto:ramalinganc@gmail.com) (C. Ramalingan).



**Scheme 1.** Synthesis of 7-(3,6-di-tert-butyl-9H-carbazol-9-yl)-10-alkyl-10H-phenothiazine-3-carbaldehydes.

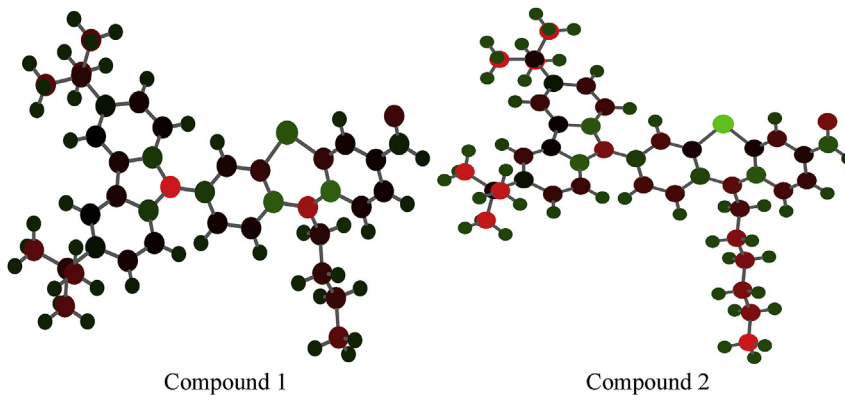


**Fig. 1.** Optimized structure and Mulliken charge distribution indicated by color code of compounds **1** and **2**.

## 2. Experimental section

### 2.1. Characterization

The melting point of the title heterocyclic carbaldehydes was measured in capillaries (open) and is un-corrected. IR spectra of the synthesized molecules were acquired on Shimadzu IR Tracer-100 in the range between 400 and 4000 cm<sup>-1</sup> utilizing KBr pellet form (resolution – 04; number of scans – 25). The spectral assignments are reported in wavenumber (cm<sup>-1</sup>). Spectra of <sup>1</sup>H and <sup>13</sup>C NMR were obtained on Bruker spectrometer (400 MHz) using chloroform-D (CDCl<sub>3</sub>) as a solvent. The values of chemical shifts are given in parts per million (ppm) from tetramethylsilane (TMS). UV–Vis spectra of the molecules have been obtained in dichloromethane (DCM), hexane, and ethanol in the region 200–800 nm and the spectrophotometer used for the same is JASCO V-650.

### 2.2. Synthesis of heterocyclic carbaldehydes **1** and **2**

#### 2.2.1. Synthesis of intermediates

The intermediates, alkylphenothiazines **4** and **5**, alkylphenothiazine carbaldehydes **6** and **7**, bromophenothiazine carbaldehydes **8** and **9**, and alkylcarbazole **11** were synthesized by employing literature methods [17–19].

#### 2.2.2. Synthesis of heterocyclic carbaldehyde **1**

In a double neck round-bottomed flask (100 mL) with water

condenser under nitrogen atmosphere, was charged bromophenothiazine carbaldehyde **8** (0.50 g, 1.38 mmol), alkylcarbazole **11** (0.39 g, 1.38 mmol), potassium carbonate (0.6 g, 4.34 mmol), copper-bronze (0.14 g, 2.16 mmol), and 18-crown-6 (0.06 g, 0.20 mmol). Then, 1,2-Dichlorobenzene (20 mL) was added using a syringe and stirred for two minutes. It was then heated to reflux and continued the same with stirring for 48 h. After cooling, it was filtered and the dark-brown filtrate-solution was collected. The insoluble material was rinsed with dichloromethane (3 × 30 mL). The rinsed solution thus obtained together with the collected dark-brown filtrate was washed with a dilute solution of aqueous ammonia followed by water. The washed dichloromethane, after drying over anhydrous magnesium sulfate, was evaporated with the help of rotary evaporator to provide a crude mixture. The pure title compound was eventually obtained upon column chromatographic separation using hexane-dichloromethane mixture (4:6). Yield: 0.56 g (73%), mp. 218–220 °C. IR (KBr, cm<sup>-1</sup>): 3055–2713 (C–H aromatic & aliphatic), 1693 (C=Oaldehyde), 1602, 1579 (C=C), 1257, 1236 (C–N), 1101 (C–S); <sup>1</sup>H NMR (400 MHz, CDCl<sub>3</sub>): δ 9.82 (s, 1H), 8.12 (d, *J* = 1.20 Hz, 2H), 7.70–7.68 (m, 1H), 7.62 (s, 1H), 7.47–7.44 (m, 2H), 7.34–7.26 (m, 4H), 7.04 (d, *J* = 6.00 Hz, 1H), 6.97 (d, *J* = 8.40 Hz, 1H), 3.97 (t, *J* = 7.20 Hz, 2H), 1.92–1.85 (m, 2H), 1.63–1.52 (m, 2H), 1.45 (s, 18H), 1.01 (t, *J* = 7.40 Hz, 3H); <sup>13</sup>C NMR (400 MHz, CDCl<sub>3</sub>): δ 190.00, 150.39, 142.94, 142.34, 139.25, 133.81, 131.31, 130.24, 128.65, 125.88, 125.69, 125.36, 124.50, 123.65, 123.30, 116.59, 116.29, 115.03, 109.12, 47.99, 34.77, 32.04, 29.74, 20.18, 13.84; Anal. Calcd for C<sub>37</sub>H<sub>40</sub>N<sub>2</sub>OS: C, 79.24; H, 7.19; N, 5.00; S, 5.72. Found:

**Table 1**Selected bond lengths and bond angles of compounds **1** and **2**.

Bond length	<b>1</b>	<b>2</b>	Expt	Bond length	<b>1</b>	<b>2</b>	Expt
Bond angle	<b>1</b>	<b>2</b>	Expt	Bond angle	<b>1</b>	<b>2</b>	Expt
C1–C2	1.391	1.391	1.398 (18)	C19–C20	1.393	1.393	1.366 (4)
C1–C14	1.413	1.409	1.393 (18)	C20–C21	1.417	1.417	1.411 (4)
C2–C3	1.400	1.402	1.395 (18)	C21–C22	1.399	1.399	1.385 (4)
C3–C4	1.407	1.407	1.387 (18)	C21–C34	1.544	1.544	1.517 (4)
C3–C15	1.464	1.466	—	C22–C23	1.402	1.402	1.397 (3)
C4–C5	1.383	1.383	1.391 (18)	C23–C24	1.452	1.452	1.442 (4)
C5–S6	1.838	1.845	1.761 (13)	C24–C25	1.401	1.402	1.394 (3)
C5–C14	1.417	1.414	1.403 (18)	C24–C29	1.417	1.417	1.398 (3)
S6–C7	1.835	1.842	1.766 (14)	C25–C26	1.399	1.399	1.379 (3)
C7–C8	1.391	1.391	1.389 (18)	C26–C27	1.417	1.417	1.411 (4)
C7–C12	1.407	1.404	1.400 (18)	C26–C30	1.545	1.545	1.523 (4)
C8–C9	1.401	1.401	1.393 (2)	C27–C28	1.393	1.393	1.371 (4)
C9–C10	1.397	1.400	1.384 (2)	C28–C29	1.397	1.396	1.372 (4)
C9–N17	1.423	1.424	—	C30–C31	1.552	1.545	1.524 (4)
C10–C11	1.394	1.394	1.390 (2)	C30–C32	1.545	1.552	1.520 (4)
C11–C12	1.408	1.405	1.394 (18)	C30–C33	1.553	1.552	1.539 (4)
C12–N13	1.426	1.426	1.395 (17)	C34–C35	1.545	1.552	1.514 (4)
N13–C14	1.411	1.412	1.393 (16)	C34–C36	1.552	1.552	1.520 (4)
N13–C38	1.482	1.481	—	C34–C37	1.552	1.545	1.541 (4)
C15–O16	1.243	1.242	—	C38–C39	1.544	1.539	—
N17–C18	1.410	1.410	1.376 (4)	C39–C40	1.540	1.537	—
N17–C29	1.410	1.410	1.380 (4)	C40–C41	1.536	1.538	—
C18–C19	1.397	1.397	1.382 (4)	C41–C42	—	1.539	—
C18–C23	1.416	1.417	1.400 (3)	C42–C43	—	1.536	—
Bond angle	<b>1</b>	<b>2</b>	Expt	Bond angle	<b>1</b>	<b>2</b>	Expt
C2–C1–C14	121.2	120.7	120.8 (12)	C20–C21–C22	118.0	118.0	117.3 (3)
C1–C2–C3	120.9	120.8	119.7 (12)	C20–C21–C34	119.3	119.3	119.5 (3)
C2–C3–C4	118.4	118.9	119.6 (12)	C22–C21–C34	122.7	122.7	123.2 (3)
C2–C3–C15	120.8	120.5	—	C21–C22–C23	120.5	120.5	120.9 (2)
C4–C3–C15	120.8	120.6	—	C18–C23–C22	119.9	119.8	119.3 (3)
C3–C4–C5	120.7	120.2	120.7 (12)	C18–C23–C24	107.0	107.0	106.9 (2)
C4–C5–S6	118.2	120.0	118.3 (10)	C22–C23–C24	133.1	133.1	133.8 (2)
C4–C5–C14	121.6	121.4	120.2 (12)	C23–C24–C25	133.1	133.1	134.3 (2)
S6–C5–C14	119.9	118.5	121.3 (10)	C23–C24–C29	107.1	107.0	106.8 (2)
C5–S6–C7	98.0	96.7	100.8 (6)	C25–C24–C29	119.8	119.8	118.8 (3)
S6–C7–C8	118.1	120.1	118.5 (10)	C24–C25–C26	120.5	120.5	121.4 (2)
S6–C7–C12	120.1	118.4	121.2 (10)	C25–C26–C27	118.0	118.1	116.9 (3)
C8–C7–C12	121.6	121.5	120.2 (12)	C25–C26–C30	122.6	122.7	123.2 (2)
C7–C8–C9	120.6	120.1	120.4 (13)	C27–C26–C30	119.3	119.3	119.8 (3)
C8–C9–C10	118.6	119.1	119.5 (13)	C26–C27–C28	122.8	122.8	123.4 (3)
C8–C9–N17	120.5	120.3	—	C27–C28–C29	118.0	117.9	117.7 (3)
C10–C9–N17	120.9	120.6	—	N17–C29–C24	108.9	108.9	108.3 (3)
C9–C10–C11	120.5	120.4	120.4 (13)	N17–C29–C28	130.2	130.2	130.0 (3)
C10–C11–C12	121.6	121.0	120.5 (13)	C24–C29–C28	120.9	120.9	121.7 (3)
C7–C12–C11	116.9	117.9	118.9 (12)	C26–C30–C31	109.7	112.3	112.2 (2)
C7–C12–N13	121.9	120.6	121.5 (12)	C26–C30–C32	112.3	109.7	108.8 (2)
C11–C12–N13	121.1	121.5	119.6 (12)	C26–C30–C33	109.6	109.6	110.3 (2)
C12–N13–C14	122.6	119.6	123.4 (11)	C31–C30–C32	108.0	108.0	108.6 (3)
C12–N13–C38	118.3	119.1	—	C31–C30–C33	109.2	108.0	106.8 (2)
C14–N13–C38	118.7	120.1	—	C32–C30–C33	108.0	109.2	110.1 (3)
C1–C14–C5	117.1	117.9	118.8 (12)	C21–C34–C35	112.3	109.6	111.1 (3)
C1–C14–N13	121.2	121.8	119.7 (11)	C21–C34–C36	109.6	109.7	113.1 (3)
C5–C14–N13	121.8	120.2	121.5 (12)	C21–C34–C37	109.7	112.3	108.9 (3)
C3–C15–O16	124.8	124.7	—	C35–C34–C36	108.0	109.3	109.0 (3)
C9–N17–C18	126.0	126.0	—	C35–C34–C37	108.0	108.0	109.1 (3)
C9–N17–C29	125.9	125.9	—	C36–C34–C37	109.3	108.0	105.4 (3)
C18–N17–C29	108.0	108.1	—	N13–C38–C39	116.9	113.1	—
N17–C18–C19	130.2	130.2	130.6 (3)	C38–C39–C40	111.5	113.7	—
N17–C18–C23	108.9	108.9	108.2 (3)	C39–C40–C41	113.0	113.1	—
C19–C18–C23	120.9	120.9	121.1 (3)	C40–C41–C42	—	113.4	—
C18–C19–C20	118.0	117.9	118.1 (3)	C41–C42–C43	—	113.2	—
C19–C20–C21	122.8	122.8	123.3 (3)	—	—	—	—

C, 79.43; H, 7.22; N, 4.96; S, 5.69.

**2.2.3. Synthesis of heterocyclic carbaldehyde **2****

A mixture of bromophenothenothiazine carbaldehyde **9** (0.54 g, 1.38 mmol), alkylcarbazole **11** (0.39 g, 1.38 mmol), potassium carbonate (0.60 g, 4.34 mmol), copper-bronze (0.14 g, 2.16 mmol), and 18-crown-6 (0.06 g, 0.20 mmol) in 1,2-dichlorobenzene (20 mL)

gave the title compound by adopting the above method. Yield: 0.54 g (67%), mp. 227–229 °C. IR (KBr, cm<sup>-1</sup>): 3055–2713 (C–H aromatic & aliphatic), 1693 (C=O aldehyde), 1602, 1579 (C=C), 1255, 1197 (C–N), 1143 (C–S); <sup>1</sup>H NMR (400 MHz, CDCl<sub>3</sub>): δ 9.81 (s, 1H), 8.13 (d, J = 1.60 Hz, 2H), 7.68 (d, J = 2.00 Hz, 1H), 7.61 (s, 1H), 7.46–7.44 (m, 2H), 7.31–7.25 (m, 4H), 7.02 (d, J = 8.40 Hz, 1H), 6.94 (d, J = 8.40 Hz, 1H), 3.94 (t, J = 7.20 Hz, 2H), 1.91–1.87 (m, 2H), 1.61–1.59 (m, 2H),

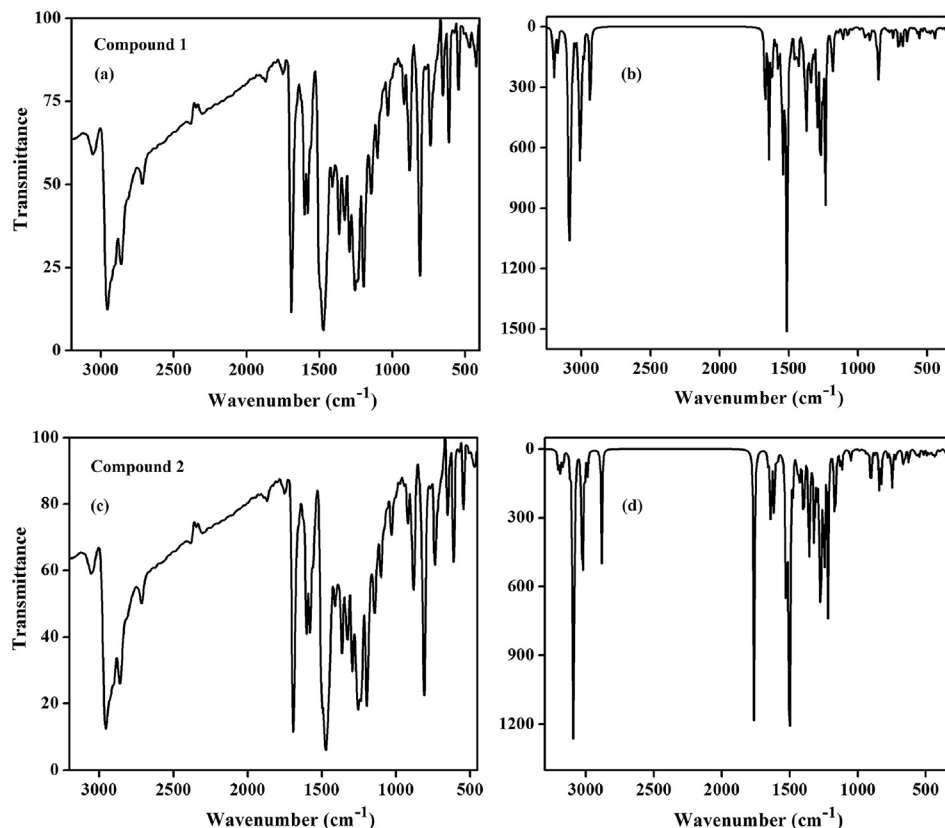


**Fig. 2.** (a) FT-IR spectrum of compound **1** (b) Simulated FT-IR spectrum of compound **1** (c) FT-IR spectrum of compound **2** (d) Simulated FT-IR spectrum of compound **2**.

1.46 (s, 18H), 1.49–1.32 (m, 4H), 0.90 (t,  $J = 4.40$  Hz, 3H);  $^{13}\text{C}$  NMR (400 MHz,  $\text{CDCl}_3$ ):  $\delta$  190.02, 150.38, 142.94, 142.31, 139.25, 133.79, 131.29, 130.26, 128.63, 125.88, 125.67, 125.35, 124.46, 123.66, 123.31, 116.60, 116.30, 115.02, 109.13, 48.30, 34.77, 32.06, 31.45, 26.79, 26.60, 22.63, 14.05; Anal. Calcd for  $\text{C}_{39}\text{H}_{44}\text{N}_2\text{OS}$ : C, 79.55; H, 7.53; N, 4.76; S, 5.45. Found: C, 79.81; H, 7.61; N, 4.73; S, 5.43.

### 2.3. Computational details

The theoretical calculations of the synthesized molecules have been performed utilizing DFT-B3LYP method with a basis set 6-311++G(d,p)[Gaussian 09 program package] [20]. The DFT (density functional theory - gradient corrected) with the Becke3 (B3 - three parameter hybrid functional) for the exchange part and the LYP (Lee-Yang-Parr) correlation function [21], agreed as an approach of cost-effective, have been adopted for the calculation of energies of vibrational frequencies and optimized structures. The frequencies computed at the aforementioned levels restrain systematic errors which are known. To bring the theoretical frequencies in close proximity to the experimental values, the scaling factor value [22] of 0.96 has been used. UV–Vis spectra for both gas and solution phases were computed by time dependent-DFT with a basis set B3LYP/6-311++G(d,p). NMR chemical shifts were computed at B3LYP/6-311++G(2d,p) level utilizing the method of Gauge Independent Atomic Orbital (GIAO) [22].

## 3. Results and discussion

### 3.1. Synthesis

The schematic representation for the synthesis of heterocyclic

carbaldehydes **1** and **2** is furnished in **Scheme 1**. Alkylphenothiazine carbaldehydes **6** and **7** were synthesized from commercially available phenothiazine **3** by alkylation using respective alkyl halides under basic condition followed by Vilsmeier-Haack reaction using phosphorous oxychloride and N,N-dimethylformamide. Bromination of **6** and **7** utilizing bromine as a brominating agent provided key intermediates bromophenothiazine carbaldehydes **8** and **9**, respectively. At the same time, alkyl carbazole **11** was synthesized from commercially available carbazole **10** employing alkylation reaction with alkyl halide in the presence of Lewis acid. Copper-bronze catalyzed Ullman type coupling reaction between the carbaldehyde intermediates **8** and **9** and the alkyl carbazole eventually afforded the title heterocyclic carbaldehydes **1** and **2**, respectively in good yields (73% and 67%, respectively) and the structures were confirmed on the basis of  $^1\text{H}$  NMR,  $^{13}\text{C}$  NMR, FT-IR, and micro analysis.

### 3.2. Molecular structure

The ground state optimized structure of the heterocyclic carbaldehydes **1** and **2** has been attained by the method of B3LYP/6-311++G(d,p) and is furnished in **Fig. 1**. As shown in the figure, the molecular structure of the parent PTZ structural motif has a typical butterfly form. The presence of carbaldehyde and CZ moieties on the 3- and 7- positions, respectively of the PTZ core influences this form to a little further extent. All the bond angles and bond lengths in the computed ones are in-lined with similar compounds 1-(10H-phenothiazin-2-yl)ethanone [23] and 3,6-di-*tert*-butyl-9H-carbazole [CCDC No. 1480917]. The optimized C–C bond lengths in the CZ and PTZ moieties fall in the range between 1.383 Å and 1.466 Å, which are in good accord with the bond

**Table 2**Mulliken atomic charges of compounds **1** and **2**.

Atom	<b>1</b>	<b>2</b>	Atom	<b>1</b>	<b>2</b>
C1	-0.1647	-0.1325	H42/H44	0.1835	0.1790
C2	-0.1290	-0.1388	H43/H45	0.1632	0.1652
C3	-0.0911	-0.0877	H44/H46	0.1915	0.1935
C4	-0.1245	-0.1282	H45/H47	0.1944	0.1941
C5	-0.3233	-0.3135	H46/H48	0.1795	0.1809
S6	0.3937	0.3861	H47/H49	0.1821	0.1709
C7	-0.3255	-0.3088	H48/H50	0.1259	0.1268
C8	-0.1705	-0.1750	H49/H51	0.1769	0.1739
C9	0.2760	0.2760	H50/H52	0.1485	0.1481
C10	-0.1345	-0.1392	H51/H53	0.1753	0.1752
C11	-0.1512	-0.1133	H52/H54	0.1756	0.1754
C12	0.4187	0.3698	H53/H55	0.1467	0.1473
N13	-0.8148	-0.8094	H54/H56	0.1718	0.1719
C14	0.4396	0.4028	H55/H57	0.1789	0.1794
C15	0.1536	0.1532	H56/H58	0.1695	0.1705
O16	-0.3626	-0.3609	H57/H59	0.1691	0.1804
N17	-1.0079	-1.0077	H58/H60	0.1795	0.1789
C18	0.2709	0.2711	H59/H61	0.1806	0.1691
C19	-0.0660	-0.0660	H60/H62	0.1704	0.1698
C20	-0.1533	-0.1532	H61/H63	0.1770	0.1770
C21	0.0890	0.0893	H62/H64	0.1688	0.1692
C22	-0.0020	-0.0020	H63/H65	0.1692	0.1691
C23	-0.1847	-0.1828	H64/H66	0.1801	0.1698
C24	-0.1856	-0.1847	H65/H67	0.1793	0.1773
C25	-0.0017	-0.0015	H66/H68	0.1705	0.1691
C26	0.0887	0.0890	H67/H69	0.1705	0.1784
C27	-0.1529	-0.1529	H68/H70	0.1783	0.1701
C28	-0.0651	-0.0654	H69/H71	0.1691	0.1692
C29	0.2722	0.2722	H70/H72	0.1700	0.1804
C30	-0.2528	-0.2528	H71/H73	0.1773	0.1706
C31	-0.4634	-0.5048	H72/H74	0.1692	0.1791
C32	-0.5050	-0.4635	H73/H75	0.2071	0.1860
C33	-0.4632	-0.4635	H74/H76	0.2077	0.1987
C34	-0.2531	-0.2530	H75/H77	0.1857	0.1955
C35	-0.5049	-0.4632	H76/H78	0.1874	0.1763
C36	-0.4632	-0.4635	H77/H79	0.1753	0.1617
C37	-0.4634	-0.5047	H78/H80	0.1760	0.2097
C38	-0.2515	-0.2091	H79/H81	0.1814	0.1682
C39	-0.3222	-0.3520	H80/H82	0.1771	0.1620
C40	-0.3507	-0.3204	H81/H83	0.1767	0.1693
C41	-0.5146	-0.3256	-/H84	—	0.1754
C42	—	-0.3440	-/H85	—	0.1750
C43	—	-0.5163	-/H86	—	0.1725
			-/H87	—	0.1706

lengths obtained from experimental results. The computed bond lengths of C–S and C–N in PTZ ring are 1.424 Å and 1.842 Å, respectively (deduced by B3LYP method). On comparing with experimental values [24], these are deviated from 0.03 to 0.07 Å.

The important bond angles and bond lengths are provided in Table 1. As can be seen, some of the bond lengths and bond angles are longer/larger and this may probably be due to the larger basis set preferred.

### 3.3. Vibrational analysis

The experimental and computed FT-IR spectra of molecules **1** and **2** are given in Fig. 2. The vibrational frequencies resulted from experimental and computational ones [B3LYP/6-311++G(d,p)] in addition to their relative intensities and feasible assignments of molecules **1** and **2** are summarized in Supplementary Tables S1 and S2, respectively. A general observation is that the frequencies obtained from computational calculations are in good concord with the ones acquired from experimental outcomes.

The modes of stretching vibrations in the aromatic and heteroaromatic ring systems are receptive to various substituents and the vibrations of the aromatic rings observed strongly in the area 1630–1480 cm<sup>-1</sup> [25]. In this investigation, the frequencies observed in the region 1602–1471 cm<sup>-1</sup> for the compounds **1** and **2** are assigned to stretching vibrations of C–C. The results of computational study using B3LYP/6-311++G(d,p) method imply that the vibrations resulted in the region 1605–1470 cm<sup>-1</sup> are corresponds to the same. As it is known, the in-plane bending vibrations of C–C–C are usually occur at less than 700 cm<sup>-1</sup> and these vibrational bands are reasonably sensitive to alteration in the position as well as nature of the substituents [26]. In the molecules **1** and **2**, the experimental C–C–C out-of-plane and in-plane bending vibrations are observed in the area 810–504 cm<sup>-1</sup> and the results of C–C–C out-of-plane and in-plane bending vibrations obtained from computational analysis are also in harmony with the experimental ones (Supplementary Tables S1 and S2).

The C–H stretching vibrations of aromatic region are usually anticipated to emerge in the area 3100–3000 cm<sup>-1</sup> [27] and the character of substituents do not usually influence the absorption bands much in the region. In accordance with the aforementioned statement, the absorption bands resulted at 3055 cm<sup>-1</sup> for both the compounds are assigned to aromatic C–H stretching vibrations. The obtained experimental aromatic C–H stretching vibrations exhibit good accord with the computational results, observed at 3065 and 3056 cm<sup>-1</sup> in B3LYP method. Literature report also support for the observed frequencies of C–H stretching vibrations [28]. It has been documented that the bending vibrations of C–H out-of-plane and in-plane modes commonly lie between 800 and 450 cm<sup>-1</sup> and 1300–1000 cm<sup>-1</sup> [27], respectively. In the current

**Table 3**Electronic transition of compounds **1** and **2** in gas and solution phase.

Solvent	Compound 1				Compound 2					
	Experimental		Calculated		Experimental		Calculated			
	λ (nm)	Abs.	λ (nm)	E (eV)	f	λ (nm)	Abs.	λ (nm)	E (eV)	f
Gas			421.24 (149 → 151)	2.9433	0.1789			409.82 (156 → 159)	3.0253	0.1071
			369.55 (149 → 151)	3.3550	0.0299			360.59 (153 → 159)	3.4383	0.0696
DCM			349.65 (145 → 151)	3.5459	0.0022			348.59 (153 → 159)	3.5567	0.0107
	399	0.1301	428.37 (149 → 151)	2.8943	0.2741	389.5	0.1128	415.31 (157 → 159)	2.9853	0.1882
	351	0.1337	369.50 (149 → 151)	3.3555	0.0376	333	0.1528	363.40 (157 → 159)	3.4118	0.0891
EtOH	294.5	0.7316	341.13 (148 → 151)	3.6345	0.0002	296.5	0.5308	340.11 (156 → 159)	3.6454	0.0003
	403.5	0.1263	427.70 (149 → 151)	2.8988	0.2746	388	0.1117	414.77 (157 → 159)	2.9892	0.1915
	353	0.1318	368.42 (149 → 151)	3.3653	0.0361	332	0.1553	362.61 (157 → 159)	3.4192	0.0862
Hexane	297.5	0.7385	339.48 (148 → 151)	3.6522	0.0002	296	0.5266	338.47 (156 → 159)	3.6631	0.0003
	405	0.1166	427.33 (149 → 151)	2.9014	0.2478	381	0.0528	414.48 (157 → 159)	2.9913	0.1593
	350.5	0.1136	371.26 (149 → 151)	3.3396	0.0386	346	0.1089	363.79 (157 → 159)	3.4081	0.0923
	296.5	0.6722	345.65 (148 → 151)	3.5870	0.0001	296.5	0.4776	344.73 (156 → 159)	3.5966	0.0004

experimental study, the weak to strong bands resulted at 651–572 cm<sup>-1</sup> and 1236–1197, 1143 cm<sup>-1</sup> are allocated to bending vibrations of C–H out-of-plane and in-plane modes, respectively. The corresponding absorptions as a result of computational studies are noted at 1230–1192, 1163, 1149 as well as 651–596 cm<sup>-1</sup>, which are in well accord with the results of experimental ones.

In general, C–H stretching vibrations of alkyl groups/chain occur at comparatively lower frequencies than those present in the aromatic rings, i.e. 2970–2840 cm<sup>-1</sup> [29]. In the FT-IR spectra of molecules **1** and **2**, the C–H stretching vibrations are observed at 2956–2713 cm<sup>-1</sup> as weak and medium bands whereas in the corresponding theoretical FT-IR spectra, these vibrations of C–H stretching modes are visualized in the area 2957–2769 cm<sup>-1</sup>. Hence, the computational and experimental results are well comparable to each other. Further, all these assignments are in harmony with the results of literature as well [28]. It is obvious that an isopropyl group or *tert*-butyl moiety usually gives distinctive band in the symmetric CH<sub>3</sub> bending region. In the case of compounds **1** and **2**, strong to weak bands observed at 1363–1325/1294 cm<sup>-1</sup> are assigned to *tert*-butyl groups. The wave numbers resulted from computational analysis, 1365–1330 and 1300/1292 cm<sup>-1</sup> are best correlated with the experimental ones.

The vibrations of C=O stretching modes furnish characteristic clear bands in the FT-IR, and the intensity of these clear bands could be increased owing to either the formation of hydrogen bonds or conjugation. Normally, the C=O stretching vibrations of carbaldehyde functionality are appears in the region 1760–1720 cm<sup>-1</sup> [30]. In the present experimental study, the aldehyde carbonyl stretching mode for compounds **1** and **2** are observed at 1693 cm<sup>-1</sup> while the B3LYP calculations give this mode at 1692 and 1672 cm<sup>-1</sup>. The experimentally observed C=O stretching vibrations of

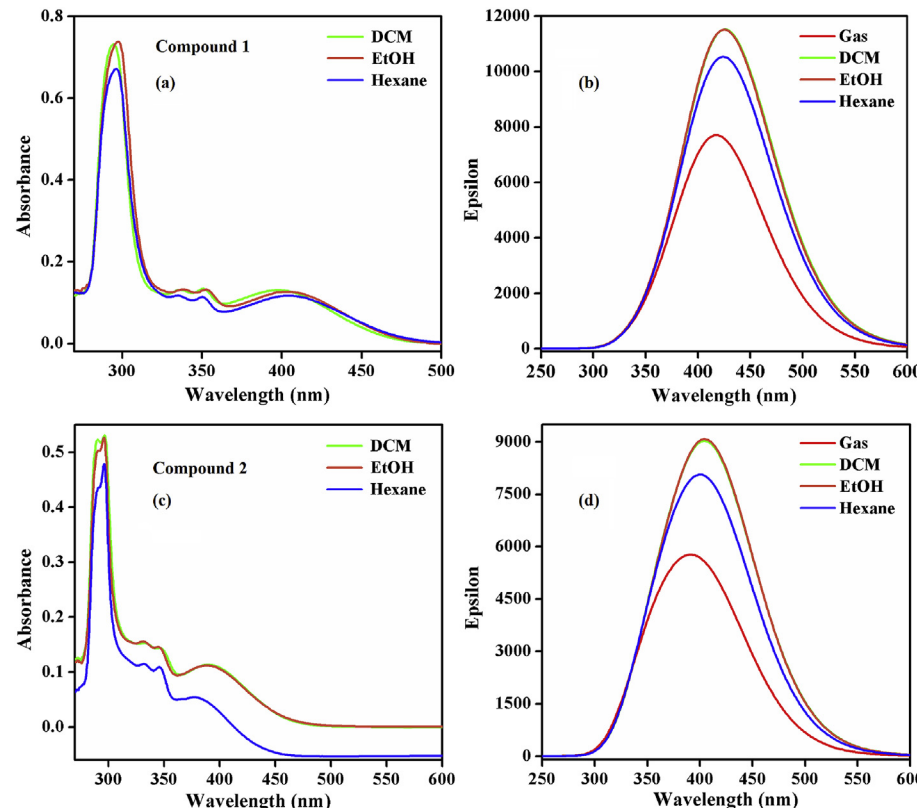
carbaldehyde functionality and the counterpart resulted from computational study are well comparable to each other.

Normally, the assignment for carbon-heteroatom stretching vibrations such as C–S and C–N ones is intricate in the infrared, since the band is of inconsistent intensity and also may be noted in the broad range between 1220 and 1080 cm<sup>-1</sup> [28,31]. The C–N and C–S moieties are less polar than carbonyl group and have noticeably weaker bands. The C–N and C–S absorptions are resulted in the FT-IR spectra of compounds **1/2** at 1257/1255 and 1029/920 cm<sup>-1</sup>, respectively and the corresponding computed values for compounds **1/2** lie at 1262/1620 and 1024/926 as well as 1029/915 cm<sup>-1</sup>, respectively. As can be seen from the above absorptions, the theoretically computed results are in-line with the experimental ones.

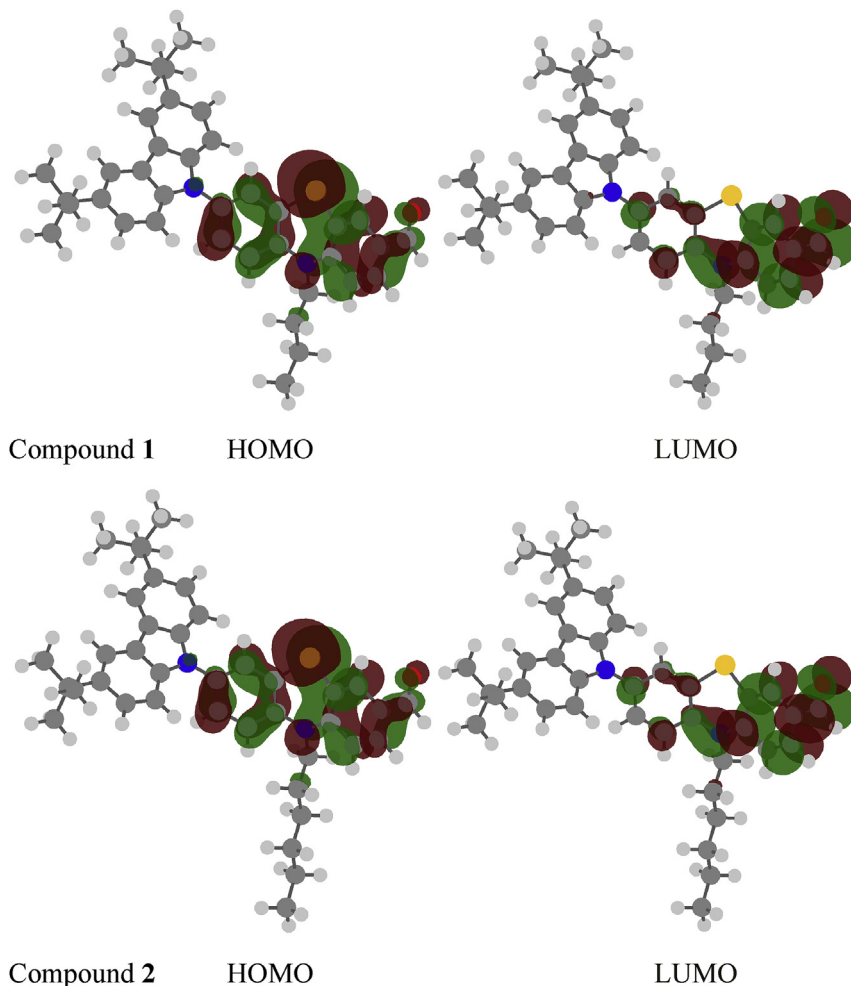
The linear regressions between the experimental and theoretical wavenumbers obtained for compounds **1** and **2** are presented in Supplementary Fig. S1. The minimal RMS (0.999) deviation confirms the reliability of the assignments of the fundamental modes of the compounds **1** and **2**.

### 3.4. Analysis of Mulliken population

The atomic charges (total) of compounds **1** and **2** acquired by Mulliken population analysis with DFT-B3LYP/6-311++G(d,p) method have been given in Table 2. Atomic charges have been utilized to illustrate the process of equalization of electro negativity and transfer of charge in chemical reactions [32]. The result shows that most of the carbon atoms in the molecules (**1** and **2**) accommodate higher negative charges lead to a reorganization of electron density. The carbon atoms such as C9, C12, C14, C15, C18, C21, C26 and C29, which are directly connected to the electronegative atoms,



**Fig. 3.** (a) UV–Vis spectrum of compound **1** (b) Simulated UV–Vis spectrum of compound **1** (c) UV–Vis spectrum of compound **2** (d) Simulated UV–Vis spectrum of compound **2**.

**Fig. 4.** HOMO-LUMO plots of compounds **1** and **2**.**Table 4**  
HOMO-LUMO energies of compounds **1** and **2**.

Parameters (eV)	<b>1</b>	<b>2</b>
HOMO	-6.7562	-6.8667
LUMO	-5.2470	-5.2590
ΔE	1.5092	1.6077
HOMO-1	-7.9233	-7.8994
LUMO+1	-5.0838	-5.0840
ΔE1	2.8395	2.8154
HOMO-2	-8.3546	-8.2901
LUMO+2	-4.1683	-4.1825
ΔE2	4.1863	4.1076

hold elevated positive charge and as a result of the same, they become greater acidic. Further, in both the compounds **1** and **2**, the positive charges are distributed on hydrogen atoms of the CZ and PTZ moieties. The better symbolized graphical appearance of the results is shown in Fig. 1.

### 3.5. UV-Vis spectral analysis

The method of TD-DFT with the basis set B3LYP/6-311++G(d,p) has been utilized to compute the UV-Vis spectra of the molecules **1** and **2**. The wavelengths, excitation energies, band gap energies and oscillator strengths as well as the pertinent parameters of

molecules **1** and **2** in both vacuum as well as solvent phase have been furnished in Table 3. The UV-Vis spectra (experimental) of the molecules **1** and **2** have been recorded in dichloromethane, ethanol and hexane. Fig. 3 proves the calculated and experimental UV-Vis spectra of the molecules **1** and **2**.

From Fig. 3, the observed two characteristic bands in the wavelengths at ~400 and ~290 nm for all the three solvents (dichloromethane, ethanol and hexane) have been assigned to  $n \rightarrow \pi^*$  and  $\pi \rightarrow \pi^*$  transitions of the molecules **1** and **2**. The former absorption bands at ~400 nm in all the solvents are due to the  $n \rightarrow \pi^*$  transition of the carbaldehyde functional moiety and the later ones with strong intense band at ~290 nm are due to  $\pi \rightarrow \pi^*$  transitions of CZ and PTZ structural motifs. The absorption intensities are slightly increased in non-polar solvents (Fig. 3). This hyperchromic shift is probably due to neither hydrogen bonding nor the nonpoints to the deprotonation of the compounds in the solution state. The experimental  $\lambda_{\max}$  values and the computed  $\lambda$  excitation wavelengths agree reasonably well above 300 nm.

### 3.6. Analysis of HOMO-LUMO

The molecular orbitals (MOs) are significant quantum chemical factors for the determination of interaction of a molecule with other species and also for characterization of chemical reactivity, global softness and hardness and, molecule's kinetic stability [33].

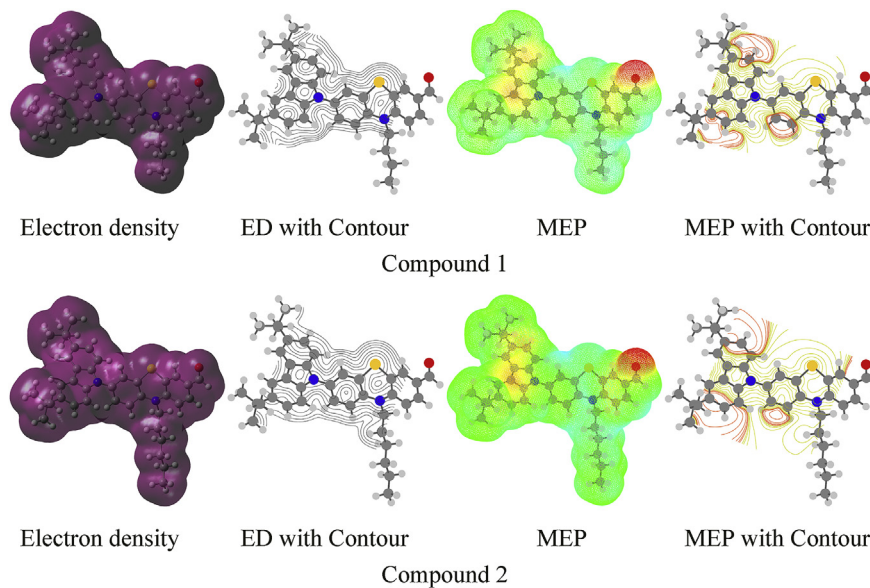


**Fig. 5.** Electron density and MEP with their contour of compounds **1** and **2**.

Energy difference between LUMO and HOMO orbitals is one of the vital factors for the determination of molecules' excitability; lesser the energy, there is a decrease in the topological resonance energy [34]. Here, six important molecular orbital energies have been examined for compounds **1** and **2**: the ground state, first and second highest occupied and lowest unoccupied molecular orbitals which are designated as HOMO, LUMO, HOMO-1, LUMO+1, HOMO-2, and LUMO+2. Pictorial representations and related data of these molecular orbitals are furnished in Fig. 4 and Table 4, respectively. As per B3LYP/6-311++G(d,p) calculation, the band-gap energies ( $\Delta E$ ) of the compounds **1** and **2** are about 1.5092 and 1.6077 eV. The HOMO's are localized largely on the PTZ moiety. At the same time, the LUMO's are localized chiefly on carbaldehyde part on the PTZ ring.

### 3.7. Molecular electrostatic potential (MEP) analysis

The electrostatic potential is a dominant tool which provides insight to determine the reactive sites, intermolecular association and physicochemical affairs and also interactions of hydrogen bonding [35]. Electron density and model of electrostatic potential of the molecules **1** and **2** (0.002 a.u isodensity surface computed) are shown in Fig. 5. From the MEP pictures, it could be seen that the isosurfaces ranges from -0.104 to +0.104 kcal/mol with dark-blue colour signifying exceedingly electron-poor regions and red-colour denoting electron rich region. As seen from the figure, the plausible reactive location of the molecules **1** and **2** are in support of electrophilic-attack. The negative province is confined on the area of oxygen atom of the carbaldehyde (O16) part of PTZ ring.

### 3.8. Nuclear magnetic resonance spectral analysis

The optimized structure of the studied molecules **1** and **2** is used to calculate the proton and carbon NMR employing DFT-B3LYP/6-311++g(2d,p) method. The theoretical chemical shifts of both the molecules are compared with their corresponding experimental NMR data, summarized in Table 5. In the experimental proton NMR, chemical shifts of aromatic ring protons are collectively resonated in the region of 8.1–6.9 ppm while in the theoretical proton NMR,

the same have been resonated in the region of 7.8–6.8 ppm. The carbaldehyde proton of both the molecules **1** and **2** is appeared in the extreme downfield region of 9.8 ppm in the experimental proton NMR due to the deshielding effect and this experimental value is comparable with that of the chemical shifts of **1** and **2** resulted from the computational calculations. Further, signals for alkyl functionalities such as n-butyl, n-hexyl, and di-*tert*-butyl of both the molecules are obtained experimentally in the range of 4.0–0.9 ppm while the same resulted theoretically in the range of 4.2–0.8 ppm.

The experimental  $^{13}\text{C}$  chemical shift values of aromatic ring carbons of CZ and PTZ structural motifs are obtained in the range between 150 and 109 ppm and these values are comparable with that of the results acquired from theoretical calculations. The chemical shift of carbonyl carbon of the molecules **1** and **2** are resonated experimentally at 190.00 and 190.02 ppm, respectively while the same theoretically obtained at 193.03 and 193.15 ppm, respectively by employing B3LYP method and these are comparable to each other. In addition, the alkyl carbons resonated in the region of 41–94–14.50 ppm and 48.30–14.05 ppm in the theoretical and experimental  $^{13}\text{C}$  NMR, respectively. On the whole, experimental and computational results of  $^1\text{H}$  NMR and  $^{13}\text{C}$  NMR of the molecules **1** and **2** imply that both the results are good to satisfactory when compared to each other. On comparing the theoretical results, slight variations noted in the experimental chemical shifts especially in the alkyl region are probably due to the effect of solvent, concentration, and temperature.

### 3.9. Non-linear optical characteristics

For investigating the relationship between non-linear optical properties (NLO) and molecular structures, the polarizabilities as well as first order hyperpolarizabilities have been calculated. It is recognized that molecules possessing superior dipole moment, molecular polarizability and first hyperpolarizability show greater non-linear optical behaviors [36]. The first hyperpolarizability ( $\beta$ ) and the hyperpolarizability components  $\beta_x$ ,  $\beta_y$  and  $\beta_z$  of compounds **1** and **2** in addition to associated characteristics ( $\mu_0$ ,  $\alpha_{\text{total}}$ , and  $\alpha_0$ ) are provided in Table 6.

**Table 5**NMR Chemical Shift of compounds **1** and **2**.

Atom	<b>1</b>		<b>2</b>		Atom	<b>1</b>		<b>2</b>	
	Calc.	Expt.	Calc.	Expt.		Calc.	Expt.	Calc.	Expt.
H48/H50	9.64	9.82	9.58	9.81	C15	193.03	190.00	193.15	190.02
H42/H44	6.77	8.12–6.97	6.84	8.13–6.94	C1	112.63	150.39–109.12	115.73	150.38–109.13
H43/H45	7.30		7.34		C2	133.85		135.86	
H44/H46	7.49		7.74		C3	130.61		132.09	
H45/H47	7.09		7.21		C4	124.65		126.57	
H46/H48	7.17		7.30		C5	131.49		136.61	
H47/H49	7.04		7.02		C7	131.94		137.58	
H49/H51	7.11		7.15		C8	124.91		126.65	
H50/H52	7.24		7.28		C9	135.95		136.55	
H51/H53	7.85		7.78		C10	125.42		126.88	
H52/H54	7.81		7.81		C11	115.45		118.77	
H53/H55	7.31		7.21		C12	143.34		141.48	
H54/H56	7.12		7.12		C14	151.13		154.92	
H55/H57	1.08	1.45	1.55	1.46	C18	139.82		140.50	
H56/H58	1.57		1.41		C19	108.17		107.69	
H57/H59	1.14		1.56		C20	125.75		124.48	
H58/H60	1.56		1.03		C21	144.95		144.45	
H59/H61	1.55		1.13		C22	114.80		114.51	
H60/H62	1.37		1.63		C23	124.68		124.25	
H61/H63	1.12		1.04		C24	124.62		124.49	
H62/H64	1.51		1.34		C25	114.57		114.49	
H63/H65	1.19		1.32		C26	144.03		144.17	
H64/H66	1.68		1.58		C27	123.67		125.14	
H65/H67	1.66		1.05		C28	107.83		107.60	
H66/H68	1.23		1.20		C29	140.32		141.11	
H67/H69	1.57		1.12		C30	41.25	47.99–34.77	41.94	48.30–34.77
H68/H70	1.05		1.53		C31	31.53		28.00	
H69/H71	1.27		1.22		C32	27.75		31.60	
H70/H72	1.37		1.60		C33	31.83		31.54	
H71/H73	1.04		1.35		C34	41.37		41.26	
H72/H74	1.35		1.61		C35	27.79		31.70	
H73/H75	3.61	3.97–1.01	4.24	3.94–0.90	C36	31.80		31.54	
H74/H76	3.67		3.76		C37	31.28		27.84	
H75/H77	2.05		1.97		C38	55.18	32.04–13.84	50.78	32.06–14.05
H76/H78	2.06		1.39		C39	30.54		30.25	
H77/H79	1.42		1.07		C40	22.75		31.07	
H78/H80	1.44		1.85		C41	14.17		35.14	
H79/H81	1.29		1.04		C42	—	—	26.85	
H80/H82	0.98		1.21		C43	—	—	14.46	
H81/H83	1.00		1.24						
–/H84	—	—	1.32						
–/H85	—	—	1.12						
–/H86	—	—	0.76						
–/H87	—	—	0.82						

The calculated values of total dipole-moment and polarizability of compounds **1** and **2** are found to be 6.871, 6.205 Debye and  $6.223 \times 10^{-23}$ ,  $6.681 \times 10^{-23}$  Debye-Ang, respectively. Nevertheless, the average value of polarizability of the synthesized compounds **1** and **2** are larger than that of *p*-nitroaniline, a typical non-linear optical material [37]. The degree of molecular hyperpolarizability ( $\beta$ ) of compounds **1** and **2** are  $3.641 \times 10^{-30}$  and  $3.205 \times 10^{-30}$ , respectively. Further, the first hyperpolarizability values of the compounds **1** and **2** are compared with urea ( $0.372 \times 10^{-30}$  esu). The hyperpolarizability values ( $\beta$ ) of compounds **1** and **2** are nearly nine times higher compared to urea [38]. In addition, the dipole-moments of compounds **1** and **2** are also greater when compared with urea (1.373 Debye). The aforementioned results imply that the molecular polarizability as well as hyperpolarizability of the synthesized compounds **1** and **2** in all coordinates are active and hence they could be utilized for the preparation of non-linear optical crystals which might generate second order harmonic waves.

#### 4. Conclusion

Two new heterocyclic molecules, 7-(3,6-di-*tert*-butyl-9*H*-carbazol-9-yl)-10-alkyl-10*H*-phenothiazine-3-carbaldehydes have been synthesized by adopting Ullman type coupling as a key step. Computational and experimental studies on the same have been made. The parameters related to the molecular structure of the title compounds are in good accord with the reported XRD results of single crystal. The vibrational frequencies obtained experimentally are compared with the theoretically calculated wave numbers and are in harmony with each other. The small energy difference between the HOMO and LUMO of the title compounds enlighten the happening of ultimate transfer of charge within the molecule. The molecular orbitals, molecular electrostatic potential surface and NLO analysis direct to the understanding of various properties of the molecules synthesized. The synthesized molecules could be utilized for the preparation of NLO crystals which might generate second order harmonic waves.

**Table 6**  
NLO properties of compounds **1** and **2**.

	<b>1</b>	<b>2</b>
Dipole moment		
$\mu_x$	−0.657	0.328
$\mu_y$	4.604	0.155
$\mu_z$	−5.058	−6.195
$\mu(D)$	6.871	6.205
Polarizability		
$\alpha_{xx}$	−241.988	−259.912
$\alpha_{yy}$	−255.484	−264.469
$\alpha_{zz}$	−270.884	−285.478
$\alpha_{\text{total}}$	$6.223 \times 10^{-23}$	$6.681 \times 10^{-23}$
$\alpha_0$	−256.1184	−269.953
Hyperpolarizability		
$\beta_{xxx}$	−37.249	−22.451
$\beta_{xxy}$	177.706	−22.417
$\beta_{xyy}$	73.474	−8.857
$\beta_{yyy}$	30.716	−2.458
$\beta_{xxz}$	−175.526	−201.511
$\beta_{xyz}$	−44.957	63.588
$\beta_{yyz}$	−40.528	−28.103
$\beta_{xz}$	70.746	−90.974
$\beta_{yz}$	66.037	55.231
$\beta_{zzz}$	−85.252	−119.298
$\beta_0$	$3.641 \times 10^{-30}$	$3.205 \times 10^{-30}$

geometry, *Adv. Funct. Mater.* **16** (2006) 1057–1066.

- [10] A. Tacca, R. Po, M. Calderaro, S. Chiaberge, L. Gila, L. Longo, P.R. Mussini, A. Pellegrino, N. Perin, M. Salvalaggio, A. Savoini, S. Spera, Ternary thiophene-X-thiophene semiconductor building blocks (X = fluorene, carbazole, phenothiazine): modulating electronic properties and electropolymerization ability by tuning the X core, *Electrochim. Acta* **56** (2011) 6638–6653.
- [11] Y.-J. Cheng, S.-H. Yang, C.-S. Hsu, Synthesis of conjugated polymers for organic solar cell applications, *Chem. Rev.* **109** (2009) 5868–5923.
- [12] M. Kalkanidis, N. Klonis, L. Tilley, L.W. Deady, Novel phenothiazine antimalarials: synthesis, antimalarial activity, and inhibition of the formation of  $\beta$ -haematin, *Biochem. Pharmacol.* **63** (2002) 833–842.
- [13] K. Pluta, B. Morak-Młodawska, M. Jelen, Recent progress in biological activities of synthesized phenothiazines, *Eur. J. Med. Chem.* **46** (2011) 3179–3189.
- [14] C. Bodea, I.A. Silberg, in: A.R. Katritzky, A.J. Boulton (Eds.), *Advances in Heterocyclic Chemistry*, vol. 9, Academic Press, New York, 1968, pp. 325–475.
- [15] K. Kubota, H. Kurebayashi, H. Miyachi, M. Tobe, M. Onishi, Y. Isobe, Synthesis and structure-activity relationships of phenothiazine carboxylic acids having pyrimidine-dione as novel histamine H(1) antagonists, *Bioorg. Med. Chem. Lett.* **19** (2009) 2766–2771.
- [16] A. Jaszczyszyn, K. Gasiorowski, P. Swiatek, W. Malinka, K. Cieslik-Boczula, J. Petrus, B. Czarnik-Matusewicz, Chemical structure of phenothiazines and their biological activity, *Pharmacol* **64** (2012) 16–23.
- [17] S.H. Kim, C. Sakong, J.B. Chang, B. Kim, M.J. Ko, D.H. Kim, K.S. Hong, J.P. Kim, The effect of N-substitution and ethylthio substitution on the performance of phenothiazine donors in dye-sensitized solar cells, *Dyes Pigments* **97** (2013) 262–267.
- [18] X. Yang, R. Lu, F. Gai, P. Xue, Y. Zhan, Rigid dendritic gelators based on oligocarbazoles, *Chem. Commun.* **46** (2010) 1088–1091.
- [19] Y. Liu, M. Nishihara, Y. Wang, Z. Hou, Pi-conjugated aromatic enynes as a single-emitting component for white electroluminescence, *J. Am. Chem. Soc.* **128** (2006) 5592–5594.
- [20] M.J. Frisch, G.W. Trucks, H.B. Schlegel, G.E. Scuseria, M.A. Robb, J.R. Cheeseman, G. Scalmani, V. Barone, B. Mennucci, G.A. Petersson, H. Nakatsuji, M. Caricato, C. Li, H.P. Hratchian, A.F. Izmaylov, J. Bloino, G. Zheng, J.L. Sonnenberg, M. Hada, M. Ehara, K. Toyota, R. Fukuda, J. Hasegawa, M. Ishida, T. Nakajima, Y. Honda, O. Kitao, H. Nakai, T. Vreven, J.A. Montgomery Jr., J.E. Peralta, F. Ogliaro, M. Bearpark, J.J. Heyd, E. Brothers, K.N. Kudin, V.N. Staroverov, R. Kobayashi, J. Normand, K. Raghavachari, A. Rendell, J.C. Burant, S.S. Iyengar, J. Tomasi, M. Cossi, N. Rega, J.M. Millam, M. Klene, J.E. Knox, J.B. Cross, V. Bakken, C. Adamo, J. Jaramillo, R. Gomperts, R.E. Stratmann, O. Yazyev, A.J. Austin, R. Cammi, C. Pomelli, J.W. Ochterski, R.L. Martin, K. Morokuma, V.G. Zakrzewski, G.A. Voth, P. Salvador, J.J. Dannenberg, S. Dapprich, A.D. Daniels, O. Farkas, J.B. Foresman, J.V. Ortiz, J. Cioslowski, D.J. Fox, Gaussian 09, Revision E.01, Gaussian, Inc., Wallingford CT, 2009.
- [21] a) C. Lee, W. Yang, R.G. Parr, Development of the Colle-Salvetti correlation-energy formula into a functional of the electron density, *Phys. Rev. B* **37** (1988) 785–789;  
b) A.D. Becke, Density-functional thermochemistry. III. The role of exact exchange, *J. Chem. Phys.* **98** (1993) 5648–5652.
- [22] a) G. Rauhut, P. Pulay, Transferable scaling factors for density functional derived vibrational force fields, *J. Phys. Chem.* **99** (1995) 3093–3100;  
b) A.P. Scott, L. Radom, Harmonic vibrational frequencies: an evaluation of Hartree-Fock, Møller-Plesset, quadratic configuration interaction, density functional theory, and semiempirical scale factors, *J. Phys. Chem.* **100** (1996) 16502–16513.
- [23] J.P. Jasinski, A.E. Pek, P.S. Nayak, B. Narayana, H.S. Yathirajan, 1-(10H-Phenothiazin-2-yl)ethanone, *Acta Crystallogr.* **E67** (2011) o430–o431.
- [24] F.H. Allen, O. Kennard, D.G. Watson, L. Brammer, A.G. Orpen, R. Taylor, Tables of bond lengths determined by X-ray and neutron diffraction. Part I. Bond lengths in organic compounds, *J. Chem. Soc. Perkin Trans. II* (1987) S1–S19.
- [25] B.H. Stuart, *Infrared Spectroscopy: Fundamentals and Applications*, John Wiley and Sons, Chichester, UK, 2004.
- [26] M.A. Palafox, Scaling factors for the prediction of vibrational spectra. I. Benzene molecule, *Int. J. Quantum Chem.* **77** (2000) 661–684.
- [27] a) A. Bree, R. Zwarch, Vibrational assignment of carbazole from infrared, Raman, and fluorescence spectra, *J. Chem. Phys.* **49** (1968) 3344–3355;  
b) W. Lao, C. Xu, S. Ji, J. You, Q. Ou, Electronic and vibrational spectra of a series of substituted carbazole derivatives, *Spectrochim. Acta Part A Mol. Biomol. Spectrosc.* **56** (2000) 2049–2060.
- [28] a) N. Meng, Y. Zhang, Y. Wang, K. Ma, J. Zhao, G. Tang, Experimental and DFT studies on the vibrational and electronic spectra and NBO analysis of 2-amino-3-(E)-(9-p-tolyl-9H-carbazol-3-yl)methyleneamino)maleonitrile, *Spectrochim. Acta Part A Mol. Biomol. Spectrosc.* **121** (2014) 494–507;  
b) K.G.V. Das, C.Y. Panicker, B. Narayana, P.S. Nayak, B.K. Sarojini, A.A. Al-Saadi, FT-IR, molecular structure, first order hyperpolarizability, NBO analysis, HOMO and LUMO and MEP analysis of 1-(10H-phenothiazin-2-yl)ethanone by HF and density functional methods, *Spectrochim. Acta Part A Mol. Biomol. Spectrosc.* **135** (2015) 162–171;  
c) Y. Wang, Y. Zhang, H. Ni, N. Meng, K. Ma, J. Zhao, D. Zhu, Experimental and DFT studies on the vibrational and electronic spectra of 9-p-tolyl-9H-carbazole-3-carbaldehyde, *Spectrochim. Acta Part A Mol. Biomol. Spectrosc.* **135** (2015) 296–306.
- [29] R.G. Strauss, H.L. Strauss, C.A. Elliger, C-H stretching modes and the structure

## Acknowledgement

Financial assistance provided by the Department of Science and Technology, New Delhi, India under Fast-Track Scheme [SR/FT/CS-149/2011] is gratefully acknowledged.

## Appendix A. Supplementary data

Supplementary data related to this article can be found at <http://dx.doi.org/10.1016/j.molstruc.2016.11.022>.

## References

- [1] Y. Tao, C. Yang, J. Qin, Organic host materials for phosphorescent organic light-emitting diodes, *Chem. Soc. Rev.* **40** (2011) 2943–2970.
- [2] K. Thevissen, A. Marchand, P. Chaltin, E.M. Meert, B. Cammee, Antifungal carbazoles, *Curr. Med. Chem.* **16** (2009) 2205–2211.
- [3] F.-F. Zhang, L.-L. Gan, C.-H. Zhou, Synthesis, antibacterial and antifungal activities of some carbazole derivatives, *Bioorg. Med. Chem. Lett.* **20** (2010) 1881–1884.
- [4] M.J. Hsu, Y. Chao, Y.H. Chang, F.M. Ho, L.J. Huang, Y.L. Huang, T.Y. Luh, C.P. Chen, W.W. Lin, Cell apoptosis induced by a synthetic carbazole compound LCY-2-CHO is mediated through activation of caspase and mitochondrial pathways, *Biochem. Pharmacol.* **70** (2005) 102–112.
- [5] H. Yan, T.C. Mizutani, N. Nomura, T. Takakura, Y. Kitamura, H. Miura, M. Nishizawa, M. Tatsumi, N. Yamamoto, W. Sugiyama, A novel small molecular weight compound with a carbazole structure that demonstrates potent human immunodeficiency virus type-1 integrase inhibitory activity, *Antivir. Chem. Chemother.* **16** (2005) 363–373.
- [6] C. Ito, S. Katsuno, M. Itoigawa, N. Ruangrungsri, T. Mukainaka, M. Okuda, Y. Kitagawa, H. Tokuda, H. Nishino, H. Furukawa, New carbazole alkaloids from clausena anisata with antitumor promoting activity, *J. Nat. Prod.* **63** (2000) 125–128.
- [7] a) F. Fungo, S.A. Jenekhe, A.J. Bard, Plastic electrochromic devices: Electrochemical characterization and device properties of a phenothiazine-phenylquinoline donor-acceptor polymer, *Chem. Mater.* **15** (2003) 1264–1272;  
b) X. Kong, A.P. Kulkarni, S.A. Jenekhe, Phenothiazine-based conjugated polymers: Synthesis, electrochemistry, and light-emitting properties, *Macromolecules* **36** (2003) 8992–8999.
- [8] D.-H. Hwang, S.-K. Kim, M.-J. Park, J.-H. Lee, B.-W. Koo, I.-N. Kang, S.-H. Kim, T. Zyung, Conjugated polymers based on phenothiazine and fluorene in light-emitting diodes and field effect transistors, *Chem. Mater.* **16** (2004) 1298–1303.
- [9] A.P. Kulkarni, X. Kong, S.A. Jenekhe, High-performance organic light-emitting diodes based on intramolecular charge-transfer emission from donor-acceptor molecules: Significance of electron-donor strength and molecular

- of n-alkyl chains. 1. Long, disordered chains, *J. Phys. Chem.* 86 (1982) 5145–5150.
- [30] G. Socrates, Infrared and Raman Characteristic Group Frequencies, Tables and Charts, third ed., Wiley, Chichester, 2001.
- [31] C.N.R. Rao, R. Venkataraghavan, The C=S stretching frequency and the “-N-C=S bands” in the infrared, *Spectrochim. Acta Part A* 18 (1962) 541–547.
- [32] a) R.S. Mulliken, Electronic population analysis on LCAO-MO molecular wave functions. I, *J. Chem. Phys.* 23 (1955) 1833–1840;  
b) R.S. Mulliken, Electronic population analysis on LCAO-MO molecular wave functions. II. Overlap populations, bond orders, and covalent bond energies, *J. Chem. Phys.* 23 (1955) 1841–1846.
- [33] I. Fleming, *Frontier Orbitals and Organic Chemical Reactions*, Wiley-Blackwell, New York, 1976.
- [34] J-I. Aihara, Reduced HOMO-LUMO gap as an index of kinetic stability for polycyclic aromatic hydrocarbons, *J. Phys. Chem. A* 103 (1999) 7487–7495.
- [35] J.S. Murray, K. Sen, *Molecular Electrostatic Potentials, Concepts and Applications*, Elsevier, Amsterdam, 1996.
- [36] M. Nakano, I. Shigemoto, S. Yamada, K. Yamaguchi, Size-consistent approach and density analysis of hyperpolarizability: second hyperpolarizabilities of polymeric systems with and without defects, *J. Chem. Phys.* 103 (1995) 4175–4191.
- [37] L-T. Cheng, W. Tam, S.H. Stevenson, G.R. Meredith, G. Rikken, S.R. Marder, Experimental investigations of organic molecular nonlinear optical polarizabilities. 1. Methods and results on benzene and stilbene derivatives, *J. Phys. Chem.* 95 (1991) 10631–10643.
- [38] K. Wu, J.G. Snijders, C. Lin, Reinvestigation of hydrogen bond effects on the polarizability and hyperpolarizability of urea molecular clusters, *J. Phys. Chem. B* 106 (2002) 8954–8958.